Evaluation of the threshold stress inducing hydride reorientation in zirconium cladding including dislocation loops using multiphase-field method

Wooseob Shin[a], *Kunok Chang*[a*]
[a]*Nuclear Engineering, The Kyung Hee Univ., Deogyoung dae-ro 1732, 17104*
[*]Corresponding author: kunok.chang@khu.ac.kr

***Keywords : Threshold stress, Hydride reorientation, Multiphase-field, Dislocation loops, MOOSE framework**

1. Introduction

Nucleation and growth mechanism is a fundamental process in the formation of solid-state materials and the initial stage of the formation of a new phase within a material [1]. It involves the formation of small, stable clusters of atoms known as nuclei and can occur through two primary mechanisms: homogeneous nucleation and heterogeneous nucleation [2].

In the zirconium-based cladding in nuclear industry, nucleation and growth of hydrides occurs [3]. Once hydrogen atoms diffuse into the cladding, they cluster together to form stable hydride nuclei and these nuclei can form homogeneously within the bulk material (intragranular hydrides) or heterogeneously at grain boundaries (intergranular hydrides), dislocations, and vacancy defects [4].

Recently, several studies have been performed for the nucleation and growth, especially, homogeneous nucleation of the zirconium hydrides and represented the effect of metastable phases (ζ, γ) on the stable phase (δ) and evaluated the threshold stress level for the single hydride and stacking structure of the hydrides [5,6].

In this study, the evaluation of threshold stress inducing hydride reorientation will be performed using the multiphase-field modeling with nucleation and growth mechanism. In addition, the effect of the dislocation loop on the nucleation of hydrides will be represented.

2. Simulation details

For the evaluation of the threshold stress, multiphase-field model developed by J. Bair, et al., [5] was utilized in this study.

2.1 Multiphase-field modeling

These equations are the governing equations used in the multiphase-field modeling:

$$\frac{\partial c}{\partial t} = \nabla \cdot \mathrm{M}\left(\nabla \frac{\delta \mathrm{F_{tot}}}{\delta c}\right) \quad (1)$$

$$\frac{\partial \eta}{\partial t} = -L \frac{\delta \mathrm{F_{tot}}}{\delta \eta} \quad (2)$$

$$\nabla \cdot \boldsymbol{\sigma} = 0 \quad (3)$$

where the c is the composition of the hydrogen in the zirconium, the η is the structural order parameter, and the σ is the stress. The total free energy, F_{tot}, is composed of the chemical free energy, gradient energy, and elastic free energy. By using the free energy, the nucleation and growth of the hydrides in the zirconium cladding will be represented.

2.1.1 Chemical free energy

In multiphase-field modeling for the zirconium hydrides, the four phases including α-Zr, $\zeta - Zr_2H$, $\gamma - ZrH$, $\delta - ZrH_{1.5}$ are used and $\epsilon - ZrH_2$ is excluded because the amount of hydrogen is not enough to form the $\epsilon - ZrH_2$ in the cladding. In the multiphase-field modeling, the chemical free energies for the four phases are used after quadratic interpolation as follows:

$$F_\alpha = 100.0\left(c - c_\alpha^{eq}\right)^2, \quad (4)$$

$$F_\zeta = \Delta G_\zeta\left(\left(c - c_\zeta^{eq}\right)^2 - 1.0\right), \quad (5)$$

$$F_\gamma = \Delta G_\gamma\left(\left(c - c_\gamma^{eq}\right)^2 - 1.0\right), \quad (6)$$

$$F_\delta = \Delta G_\delta\left(\left(c - c_\delta^{eq}\right)^2 - 1.0\right). \quad (7)$$

where the ΔG_p is the formation free energy of the phase p and c_p^{eq} is the equilibrium concentration of the phase p. In addition, double-well potential, g, and penalty function, k, for the balance between each phase were also used in the chemical free energy with the dependence on the order parameter, η. The $h(\eta)$ is the interpolation function defined as $\eta^3(6\eta^2 - 15\eta + 10)$. The ω is the height of double-well potential and p used in Eq. (8) is the penalty prefactor. Therefore, the chemical free energy was used in this study as the Eq (1).

$$F_{chem} = \Sigma h(\eta) F_p + \omega g(\eta) + p k(\eta) \quad (8)$$

The chemical free energies of each phase were plotted in the Fig. 1. In Fig. 1, the common tangent line between two different phases, g_{pq}, are also plotted.

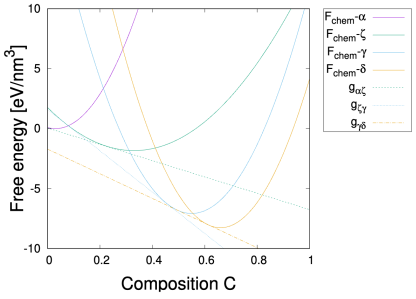

Figure 1. Chemical free energy of each phase of Zr-H.

2.1.2. Gradient energy

The gradient energy for the multiphase-field modeling is used as the tensor. The gradient coefficient, κ_{ij}, can be obtained by the relation with the height of the double-well potential ω, the thickness of the interface, l, and the interface energy, σ. The interface energy σ should be used separately with the stress, $\boldsymbol{\sigma}$. The gradient energy is used as follow:

$$F_{grad} = \frac{\kappa_{ij}}{2}|\nabla\eta|^2 \tag{9}$$

2.1.3. Elastic free energy

The elastic free energy can be obtained by using Khachaturyan's microelasticity theory [7] as follow:

$$f_{el} = \frac{1}{2}C^{tot}_{ijkl}\epsilon^{el}_{ij}\epsilon^{el}_{kl} \tag{10}$$

where the C^{tot}_{ijkl} is the total stiffness tensor interpolated using the function $h(\eta_i)$ as $C^{tot}_{ijkl} = \Sigma_i h(\eta_i)C^i_{ijkl}$ of 4 phases and the ϵ^{el}_{ij} is the elastic strain.

2.2 Dislocation dynamics

Dislocation dynamics for the dislocation loop in this study stems from the fact established by Nabarro that the dislocations can be described as a set of coherent misfitting platelet inclusions whose stress-free strain is an invariant plane strain. We set the arbitrary dislocation loop in the center of the system as the platelet with the thickness **d** to show the effect of the loop on the hydride precipitates.

$$\epsilon^{el}_{ij} = \epsilon^{tot}_{ij} - \epsilon^{misfit}_{ij} - \Sigma h(\eta_{disl})\epsilon^{disl}_{ij} \tag{11}$$

where the $\boldsymbol{\epsilon^{tot}_{ij}}$ is the total strain, $\boldsymbol{\epsilon^{misfit}_{ij}}$ is the eigenstrain from the lattice mismatch between two different phases, and the $\boldsymbol{\epsilon^{disl}_{ij}}$ is the dislocation eigenstrain which can be obtained by using the thickness **d**, burgers vector **b** and unit vector normal to the slip plane **n** as $\boldsymbol{\epsilon^{disl}_{ij} = b_i n_j/d.}$

2.3 Nucleation and growth of hydrides

The initial formation of hydrides is used as the nucleation based on the classical nucleation theory. Using the equations for the nucleation probability, critical size of the nuclei, and the corresponding critical formation free energy, we inserted the nucleation and growth mechanism in this study. The equations used in the study are as follow:

$$r^* = \frac{2\sigma}{\Delta G_v - \Delta G_{el}} \tag{12}$$

$$\Delta G^* = \frac{16\pi\sigma^3}{3(\Delta G_v - \Delta G_{el})^2} \tag{13}$$

$$J^* = ZN\beta^* \exp\left(-\frac{\Delta G^*}{k_B T}\right)\exp\left(-\frac{\tau}{t}\right) \tag{14}$$

$$P = 1 - \exp(J^* t) \tag{15}$$

where the Eq. (12) is the critical radius, Eq. (13) is the corresponding critical formation energy, Eq. (14) is the nucleation rate, and Eq. (15) is the nucleation probability. In the Eq. (14), Z is the Zeldovich correction factor, β^* is the frequency at which a critical nucleus becomes supercritical, τ is the incubation time, t is the time, and Δt is the time interval.

3. Results and Discussion

3.1. Morphology evolution of the single hydride

We showed the morphology evolution of the single hydride in Fig. 2. Once a ζ- Zr_2H precipitates in the basal plane of Zr according to the classical nucleation theory as shown in the Fig.2(a), γ- ZrH is nucleated on the ζ and phase transition occurs until the ζ disappeared totally as shown in the Fig.2(b) and (c). The δ- $ZrH_{1.66}$ is nucleated on the γ, and the phase transformation from the γ to δ phase occurs as shown in the Fig.2(d). In addition, the morphology of the hydride is changed when the γ hydride formed as the anisotropic stiffness tensor and eigenstrain. We could confirm that the formation path of δ- $ZrH_{1.66}$ is identical to the result in [5].

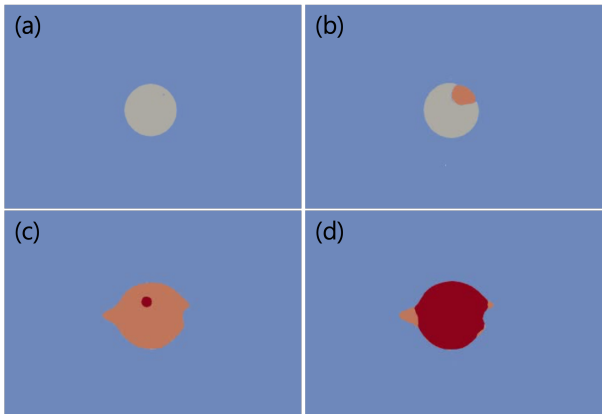

Figure 2 The evolution of single hydrides using multiphase-field modeling. (a) $\boldsymbol{\zeta - Zr_2H}$ (grey color) is nucleated first; (b) $\boldsymbol{\gamma - ZrH}$ is nucleated on the $\boldsymbol{\zeta - Zr_2H}$ and phase transition occurs; (c) $\boldsymbol{\zeta - Zr_2H}$ disappeared and $\boldsymbol{\delta - ZrH_{1.66}}$ is nucleated on the $\boldsymbol{\gamma - ZrH}$. The morphology of the hydride starts to be changed; (d) The phase transition occurs from $\boldsymbol{\gamma - ZrH}$ to $\boldsymbol{\delta - ZrH_{1.66}}$.

3.2 Threshold Stress inducing hydride reorientation

We evaluated the threshold stress using multiphase-field modeling in Fig. 3. For the applied strain, we set the displacement boundary condition which is the Dirichlet boundary condition on the displacement of the left and right boundaries. We increased the applied strain using the boundary condition, and the orientation of the hydride is drastically changed when the applied strain is over the 0.005. As a result, the threshold stress level can be evaluated at around 500MPa, obtained by multiplying the nominal value of the stiffness tensor by the applied strain imposed on the system when using multiphase-field modeling. When the phase-field modeling considering two phases ($\boldsymbol{\alpha/\delta}$) is used for the evaluation,

the threshold stress level for the single precipitate is about 1 GPa. From the comparison between two models, it is confirmed that we could obtain the lower threshold stress level when the multiphase-field modeling is used.

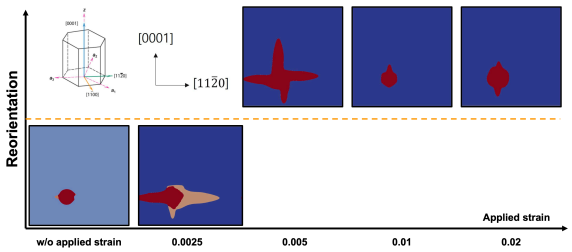

Figure 3 Threshold stress inducing hydride reorientation using multiphase-field modeling.

3.3 The effect of dislocation loop on the nucleation of the hydrides

We showed the effect of dislocation loops on the nucleation of the precipitates in Fig.4. We set the dislocation loop on the prismatic plane and basal plane as the line and circle, respectively. In addition, we increased the nucleation probability of the ζ phase to get the dislocation loop effect. We could see that the precipitates preferentially nucleate in the vicinity of the dislocation loop according to the simulation based on the classical nucleation theory. The elastic free energy induced by the dislocation affect to the critical formation energy and the nucleation probability increases around the dislocation loop in both prismatic and basal plane.

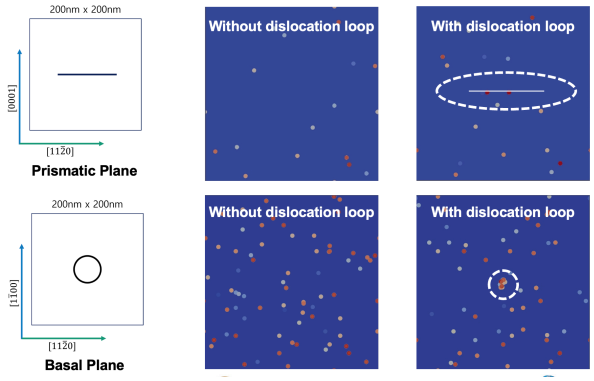

Figure 4 The effect of the dislocation loop on the nucleation of precipitates.

4. Future works

The current study doesn't include the multi hydrides for the evaluation of threshold stress and doesn't show the effect of dislocation on the morphology evolution of the hydrides. In the future works, threshold stress will be evaluated using multiphase-field modeling with dislocation loops. In addition, the multi dislocation loops including <a> loops, <c> loops are going to be considered and the effect of the dislocation loops on the morphology of the hydrides will be added to the simulation.

5. Conclusions

We performed the multiphase-field modeling to evaluate the threshold stress level generating hydride reorientation in the fuel cladding. We showed that the metastable phases (ζ, γ) influence on the morphology of stable phase (δ) and the threshold stress level using multiphase-field modeling is lower than the phase-field modeling including two phases (α, δ). In addition, we showed the hydrides preferentially nucleate in the vicinity of the dislocation loop according to the simulation based on the classical nucleation theory. However, the effect of the dislocation loop on the morphology evolution of the hydrides and the threshold stress evaluation including dislocation loop remained as the future work.

Acknowledgement

This work was also supported by the "Human Resources Program in Energy Technology" of the Korea Institute of Energy Technology Evaluation and Planning (KETEP), granted financial resources from the Ministry of Trade, Industry Energy, Republic of Korea (No. 20214000000070).

REFERENCES

[1] DA. Porter, et al., Phase Transformations in Metals and Alloys, CRC press, 2009.
[2] W. Wenkun, et al., Phase field benchmark problems for nucleation, Computational Material Science, 193, 110371, 2021.
[3] Y. Jia, and W. Han, Mechanisms of Hydride Nucleation, Growth, Reorientation, and Embrittlement in Zirconium: A Review, Materials, 16(6), 2419, 2023.
[4] Yu-Jie Jia, et al., Precipitation characteristics and distributions of subsurface hydrides in zirconium, Acta Materialia, 216, 117146, 2021.
[5] J. Bair, et al., Formation path of δ hydrides in zirconium by multiphase field modeling, Acta Materialia, 123, 235-244, 2017.
[6] T. Alireza, et al., Effects of applied load on formation and reorientation of zirconium hydrides: A multiphase field modeling study, Computational Materials Science, 192, 110367, 2021.
[7] A. G. Khachaturyan, Theory of Structural Transformations in Solids, Courier Corporation, 2013.